Pharmacogn. Mag.
A multifaceted peer reviewed journal in the field of Pharmacognosy and Natural Products
www.phcog.com | www.phcog.net

ORIGINAL ARTICLE

Characterization of PLGA-PEG *Catharanthus roseus* Nanoparticles and Assessing its Anticancer Effects in HER2-Overexpressed Breast Cancer Cells

Siti ZS, Nor Hazwani Ahmad, Shahrul Hamid

Department of Biomedical Sciences, Advanced Medical and Dental Institute, Sains@Bertam, Universiti Sains Malaysia, 13200 Kepala Batas, Penang, Malaysia

Submitted: 23-Jul-2021 Revised: 07-Mar-2022 Accepted: 11-Mar-2022 Published: 07-Jul-2022

ABSTRACT

Background: *Catharanthus roseus* (*CR*) shows promising anticancer activity. However, there is limited information on its polymeric formulation. Objectives: Therefore, current study aimed to characterize poly(lactic-co-glycolic acid (PLGA) *CR* nanoparticles and determine its effects on resistant human epidermal receptor 2 (HER2)-overexpressed breast cancer cells. **Methods:** PLGA-polyethylene glycol (PEG) *CR* nanoparticles were synthesized using the solvent displacement method and characterized using ultraviolet-visible spectroscopy (UV-VIS), Fourier-transform infrared spectroscopy (FTIR), dynamic light scattering, transmission electron microscopy (TEM), zeta potential, encapsulation efficiency, and drug release experiments. Cytotoxicity was done using 3-(4,5-dimethylthiazol-2-yl)-5-(3-carboxymethoxyphenyl)-2-(4-sulfophenyl)-2H-tetrazolium (MTS) assay. Protein expression was done with a gel image analyzer. Cell morphological changes were viewed under phase-contrast microscope. **Results:** TEM images showed the nanoparticles were spherical and size less than 100 nm. FTIR results indicated encapsulation of *CR* based on the presence of 3327 cm^{-1}, 1637 cm^{-1}, and 1066 cm^{-1} peaks. Encapsulation efficiency was >60% in both formulations. However, pluronic F68 PLGA-PEG CR nanoparticles showed a gradual release of *CR* compared with polyvinyl acetate (PVAc). The cytotoxicity assay showed that the half-maximal inhibitory concentration of the *CR* nanoparticles generated with F68 and PVAc was lower (42–58 µg/mL) on tamoxifen-resistant cells compared with parent cells (99–147 µg/mL). Further analysis using CR nanoparticles with F68 exhibited downregulation of HER2 expression and induced apoptotic features based on morphological changes. **Conclusion:** These findings suggest that PLGA-PEG nanoparticles could retain the cytotoxic effects of *CR*.

Key words: *Catharanthus roseus*, breast cancer, HER2, PLGA-PEG nanoparticles, pluronic F68, polyvinyl acetate

SUMMARY

- Findings from the present study indicated that both formulations of PLGA-PEG *CR* nanoparticles exhibited effects, however, PLGA-PEG CR G68 showed sustained release compared with PLGA-PEG CR PVAc. Furthermore, there was downregulation in the expression of fHER2 by PLGA-PEG CR F68. Further investigation is needed to confirm its underlying targeting mechanism in HER2-overexpressed breast cancer cells.

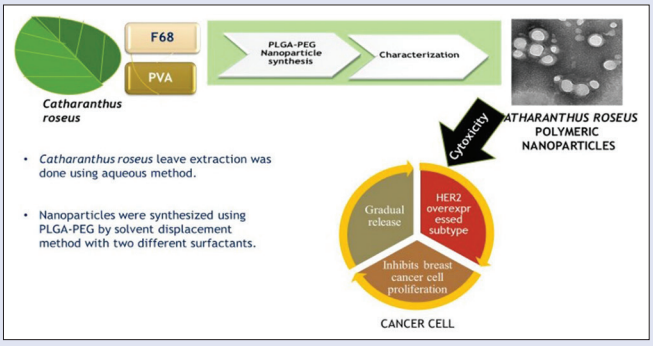

Abbreviations used: CR: Catharanthus roseus; DLS: Fourier-transform infrared spectroscopy; EE: Entrapment efficiency; F68: Pluronic F68; FTIR: Fourier-transform infrared spectroscopy; HER2: Human epidermal receptor 2; PEG: Polyethylene glycol; PLGA: poly(lactic-co-glycolic acid); PVAc: Polyvinyl acetate; rpm: Rounds per minute; TEM: Transmission electron microscopy; UV-VIS: Ultraviolet-visible spectroscopy.

Correspondence:

Dr. Shahrul Hamid,
Advanced Medical and Dental Institute, Universiti Sains Malaysia, 13200 Kepala Batas, Malaysia.
E-mail: shahrulbariyah@usm.my

DOI: 10.4103/pm.pm_338_21

Access this article online
Website: www.phcog.com
Quick Response Code:

INTRODUCTION

Human epidermal receptor 2 (HER-2)/neu is an oncogene that is amplified in human-derived breast cancer cells. A study of primary human breast cancer patients indicated that the HER-2/neu to be amplified from 2-fold to more than 20-fold in 30% of the tumors.[1] Existing therapies involve use of the anti-HER2 class of drugs, such as lapatinib, pertuzumab, and T-DM1. Nevertheless, this subtype exhibits drug resistance,[2] which highlights the need to explore new and complementary therapies.

Natural plant compounds contain numerous medicinal properties. One of the plants of interest in cancer research is *Cathranthus roseus* (*CR*) due to its anticancer potential. It is important to conserve its natural compounds to preserve their bioavailability and potency for therapeutic outcomes. Nanotechnology increasingly is being used to create carriers of chemotherapeutic drugs in clinical trials. Nanoparticles facilitate improved delivery of drugs that are less soluble in water.[3] Drug-bonded nanoparticles may increase cytotoxicity in cancer cells.[4] Studies have shown that polymeric nanoparticles are suitable drug carriers for clinical use.[5] Importantly, they exhibit promising characteristics, as they are biocompatible, non-toxic, biodegradable, stable, and provide

Cite this article as: Siti ZS, Ahmad NH, Hamid S. Characterization of PLGA-PEG *Catharanthus roseus* nanoparticles and assessing its anticancer effects in HER2-overexpressed breast cancer cells. Phcog Mag 2022;18:273-80.

controlled drug release and targeted delivery with high therapeutic efficacy.[6-9]

Synthetic polymers have higher purity and reproducibility than natural polymers. The polyester family consists of poly(lactic acid), poly(ε-caprolactone), and poly (glycolic acid). They are widely used due to their biocompatible and biodegradable properties. Among the polymers, poly (lactide-co-glycolide) (PLGA) has gained considerable interest, and the US Food and Drug Administration has given approval for use in human therapy.[10,11] Chemical characteristics of the active compound, organic solvents, polymer, and surfactant are key parameters in the synthesis of PLGA nanoparticles.[12]

Polymeric nanoparticles are versatile drug carriers that allow administration, transportation, and delivery of drugs.[13] Because nanoparticles are not taken up by the reticuloendothelial system, they accumulate at the targeted site and confer enhanced permeability and retention.[14] In addition, their biocompatible hydrophilic corona provides stealth properties. Several studies reported that their usage resulted in fewer side effects of the anticancer drugs, higher drug loading, minimized drug degradation, and thus better drug bioavailability, and increased cellular uptake.[15,16]

During the synthesis of nanoparticles, amphiphilic surfactants are used to reduce surface tension.[17] Surfactants are also used to stabilize the structure of the organic droplet. Commonly used surfactants include polyethylene glycol (PEG), Tween-80, gelatin, dextran, pluronic L-63, polyvinyl alcohol (PVA), and didodecyl dimethyl ammonium bromide.[12] Pluronics are nonionic and water-soluble materials that are used in the pharmaceutical industry.[18] In the aqueous condition, pluronics can form micelles and thus are used in the solubilization of drugs.[19] Nanoparticle preparation using the evaporation method requires use of a surfactant. Pluronic F68 is one of the most common surfactants used, and Kerleta *et al.* (2009)[20] reported that it facilitates the interaction between nanoparticles and cells.

Another commonly used type of surfactant is polyvinyl acetate (PVAc). It is a hydrophobic polymer that is widely used in the pharmaceutical industry.[15] It is used in the healthcare field because of its biocompatibility.[21] Hydrogels such as PVAc containing the carboxyl group show biocompatibility in humans.[22] It is an inert polymer and does not have adverse effects. Histological investigation of embolized rat kidneys indicated no damage to the vessel wall and no recanalization throughout the 6-month study period.[23] Previously, doxorubicin and sorafenib were coencapsulated in transferrin-functionalized PVAc core-albumin shell nanoparticles. It resulted in higher cytotoxicity (92%) than free drugs (50%) and nontargeted core-shell nanoparticles (63%).[24]

To date, anti-HER2 targeted therapies still show poor overall survival because of *de novo* or acquired resistance.[25] Hence, the development of new natural product-derived therapies using PLGA and suitable surfactants may conserve its activity and overcome resistance when used along with existing targeted therapies. Therefore, the purposes of this study was to synthesize PLGA-PEG *CR* nanoparticles with conserved bioavailability to treat resistant and parent HER2-overexpressed breast cancer cells.

MATERIALS AND METHODS

Preparation of the *CR* aqueous extract

CR leaves were collected from Bagan Ajam, Pulau Pinang. The *CR* leaves were air-dried in a universal oven (Venticell, Müchen, Germany) at 40°C, then the dried leaves were homogenized with a grinder to form a fine powder. Fifty grams of the powdered leaves were then dissolved in 1 L of distilled water, and extraction was performed at 40°C for 24 h in a shaker water bath. After extraction, the sample was then centrifuged at 14,000 rounds/min (rpm) at 25°C for 15 min. The supernatant then was transferred into a tube and freeze-dried using a freeze dryer (Eyela, Bohemia, NY, USA) at –20°C. The *CR* leaves used in this study have been previously optimized and characterized.[26] The *CR* aqueous extract was first standardized by analyzing their active compounds using liquid chromatography/time-of-flight ion trap mass (LC-TOF/MS). The data indicated the presence of 13 indole alkaloids. The summary of the compound analysis of *C. roseus* aqueous extract.

Synthesis of nanoparticles

In the synthesis of nanoparticles, two types of surfactant were studied: PVAc and pluronic F68. The nanoparticles containing the *CR* aqueous leaf extract were synthesized using the solvent displacement technique with a modified method.[27] A total of 45 mg of the polymer PLGA-PEG was added to 12.5 mL of acetone containing 5 mg of *CR* extract powder. An aqueous solution of 5 mL containing 50 mg of surfactant (either PVAc or F68) was adjusted to pH of 3.5. The organic solution was then poured into the aqueous solution under magnetic stirring for 5 min. Acetone was removed from the nanoparticle plant extract (PLGA-PEG *CR* NP) mixture using a rotary evaporator at 70°C and pressure starting at 500 pHa. The mixture was then centrifuged at a speed of 10,000 rpm for 15 min. After centrifugation, the pellet was collected and it was dried in an oven at 40°C.

Ultra violet-visible (UV-Vis) Spectroscopy

Size of the nanoparticles was characterized using UV-VIS absorption spectroscopy.[28] The absorbance of each component (solvent, polymer, surfactant, plant extract, and the mixture of nanoparticless) was analyzed using a Cary 60 UV-VIS spectrophotometer (Agilent Technologies, San Diego, CA, USA).

Fourier transform infrared (FTIR) spectroscopy

FTIR spectroscopy was used qualitatively identify functional groups present in the samples. Readings were recorded in the spectral range from 600 to 4000 cm^{-1} using a Frontier spectrometer (Perkin Elmer, Massachusettes, USA).

Dynamic light scattering (DLS)

DLS is suitable technique to measure the size and its distribution by photon correlation spectroscopy at room temperature and uses water as the suspension medium.[12] In this study, the mixture of nanoparticles was analyzed using a Zetasizer Nano ZS DLS instrument (Malvern, UK). DLS measures the size of particles and the hydrodynamics of the surface coating. Zeta potential is a measure of the charge of the synthesized nanoparticles. Data obtained were analyzed using Zetasizer Software and reported as mean of triplicate measurements.

Transmission electron microscopy (TEM)

TEM was performed for evaluating the size and morphology of the nanoparticles studied. A drop of the mixture of nanoparticles was placed onto a carbon-coated copper grid using self locking forceps and left for 3 min. Next, the excess mixture was carefully removed with paper wipes and left for 1 min. Subsequently, phosphotungstic acid solution (1%) was used for negative charge staining and left for another minute. Finally, the stain was left to dry for 5–10 min prior to viewing under the TEM (Zeiss, Oberkochen, Germany).

Percentage of encapsulation efficiency (EE)

EE is one of the most important factors that must be considered when utilizing polymer nanoparticles.[29] Therefore, the percentage of EE was studied. PLGA-PEG *CR* nanoparticles were sonicated for 1 min

and then centrifuged for 20 min at 14,000 rpm. The supernatant was used to quantify the total of free drug in the sample. Amount of *CR* extract encapsulated was determined using UV-VIS spectroscopy and was based on a standard curve. Percentage of EE was calculated as follows:

EE (%) = [(Concentration of initial drug – Concentration of free drug)/ Concentration of initial drug] × 100

Drug release

The *in vitro* drug release was measured using the dialysis method. Nanoparticles were placed into a dialysis bag, which then was sealed. It was placed in a beaker that contained 15 mL of phosphate buffer saline (PBS, pH 7.4) and continuously stirred at a speed of 100 rpm at 37°C. Next, at a specific time, 1 mL of the PBS (pH 7.4) in the beaker was withdrawn for sampling, and absorbance was measured with the UV-VIS spectrometer. One milliliter of fresh PBS (pH 7.4) was placed in the beaker to replace the withdrawn volume. Absorbance readings were plotted to generate a standard curve, and the percentage of drug release was calculated as follows:

Percentage of drug release (%) = Concentration of drug released × 100/ Concentration of drug entrapped

Cytotoxicity assay of nanoparticles

HER2-overexpressed parent cell line (UACC732) was purchased from American Type Culture Collection (ATCC). The tamoxifen-resistant cells were developed using the pulse method as reported.[30] Cells were cultured in Roswell Park Memorial Insitute (RPMI) medium (Nacalai Tesque, Kyoto, Japan) and supplemented with 10% fetal bovine serum and 1% penicillin-streptomycin (Nacalai Tesque, Kyoto, Japan). Cytotoxicity assay was done to determine the half-maximal inhibitory concentration (IC_{50}) of nanoparticles synthesized with PVAc and pluronic F68 with the CellTiter 96® AQueous nonradioactive cell proliferation assay (Promega, Madison, WI, USA). First, 3×10^3 of each type of UACC732 cells per well were seeded in a 96-well plate, with each well containing 100 µL of complete culture medium. Cells were left overnight to grow and adhere prior to treatment with nanoparticles. Cytotoxicity to UACC732 cells of both formulations of nanoparticles at different concentrations was tested for 72 h. After treatment, the cell culture medium was removed before adding 100 µL of fresh culture medium. In the next step, 20 µL of CellTiter 96® AQueous nonradioactive cell proliferation assay reagent (Promega) were placed in each well, followed by incubation at 37°C for 90 min with 5% CO_2 in an incubator. Finally, absorbance was measured at 490 nm using an ELISA microplate reader (BioTek, Shoreline, WA, US).

Western blot analysis

The expression of HER2 was studied using the Western blot method. Cells were treated with the IC_{50} of PLGA-PEG CR F68 for 3 days prior to extraction of protein. Total protein was quantified using the Bradford assay. A total of 40 µg of protein was loaded in 7.5% SDS polyacrylamide gel and electrophoresis was performed. Subsequently, protein samples were blotted to the PVDF membrane. Detection of protein expression was done using a primary antibody against HER2 (1:750 dilution). Membrane was incubated with primary antibody overnight and later treated with secondary antibody for an hour prior to viewing under Bio-Rad gel imaging system. *t*-test analysis was performed to compare mean differences between control and treatment groups using Statistical Package for Social Sciences (SPSS) software.

RESULTS

UV-VIS measurements

Synthesis of *CR* nanoparticles was performed using the solvent displacement method. However, after 24 h no color change was detected. Acetone, which acts as an organic solvent, was removed by evaporation to avoid toxicity. The UV-VIS absorption spectra of the compounds studied are provided in Figure 1. The raw extract of *CR* exhibited peak absorbance between 235 and 250 nm, and peak absorption of the positive control (the drug vinblastine) occurred at 230 nm. The F68 nanoparticles exhibited peak absorbance at 230 nm. For PVAc, the absorbance values varied from 200 to 245 nm. The result indicates that the *CR* extract was entrapped within the synthesized nanoparticles.

Measurement of particle size, polydistribution index (PDI), and zeta potential

The DLS technique is used to calculate the diameter of different types of particles dispersed in a liquid medium. A wider distribution indicates that the sample is more polydispersed.[31] Optimization of a new nanoparticle product in terms of stability and physicochemical composition requires characterization of the interfacial properties. This can be performed by measuring the zeta potential to understand the surface charge and electrical double layer of the colloidal particles.[32] Table 1 exhibits the data obtained from DLS analysis. The particle size yield was approximately 139.3 nm for nanoparticles synthesized with PVAc. The PDI value was 0.19, and the constant zeta potential was –3.44. Compared with PVAc-based nanoparticles, the size and PDI

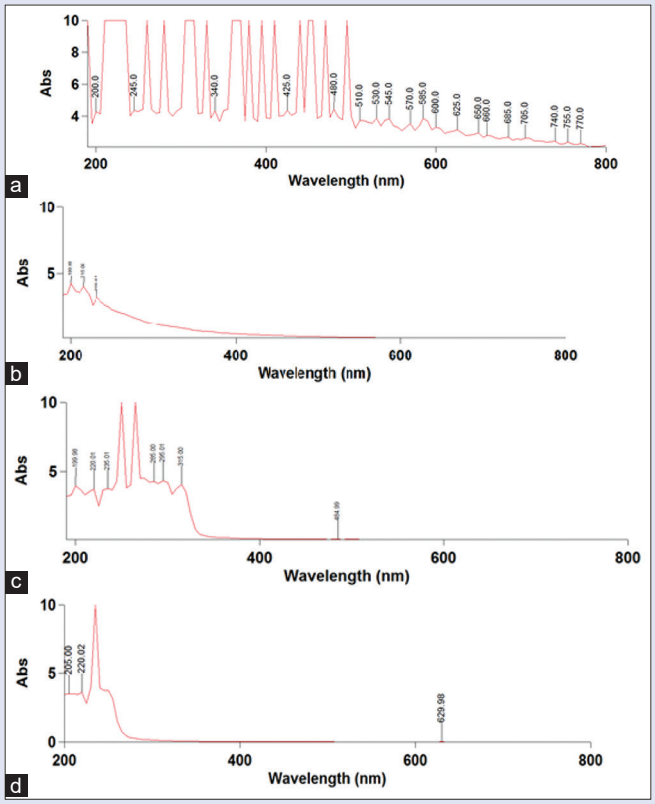

Figure 1: UV-Vis absorption spectra of different compositions used in the synthesis of nanoparticles: a) PLGA-PEG *CR* PVAc NP; b) PLGA-PEG *CR* PF68 NP; c) *CR* leaf extract; d) vinblastine as the positive control

were smaller for F68-based nanoparticles but the zeta potential value was higher.

TEM

TEM micrographs were taken to visualize the morphology and estimate the size of nanoparticles from both formulations [Figure 2]. TEM analysis showed that the mean size of nanoparticles was <100 nm. They were spherical and monodispersed. The average size was 70.09 nm (range: 36.5–124.5 nm). The average size was higher for PLGA-PEG *CR* F68 (87.31 nm) than for PLGA-PEG *CR* PVAc (70.09 nm).

FTIR analysis

FTIR provided simplicity, rapidity, and sensitivity in detecting the presence of organic constituents of the *CR* leaf extract [Figure 3]. The *CR* extract exhibited signals at 3264, 2925, 1590, 1404, and 1028 cm^{-1}. PLGA-PEG peaks were detected at 2996, 2949, 1748, 1164, and 1083 cm^{-1}. F68 showed peaks at 2883, 1341, and 1099 cm^{-1}, and PVAc exhibited peaks at 2887, 1730, 1228, 1117, 1020, and 942 cm^{-1}. Nanoparticles synthesized using pluronic F68 showed peaks at 3327, 2988, 1637, 1406, 1250, and 1066 cm^{-1}, nanoparticles synthesized with PVAc had bands at 3339, 1753, and 1637 cm^{-1}.

Percentage of EE

The percentage of drug incoperated into the nanoparticles was determined based on EE. The EE of nanoaprticles synthesized with pluronic F68 was 64%, whereas the value for PVAc nanoparticles was 60% [Table 2].

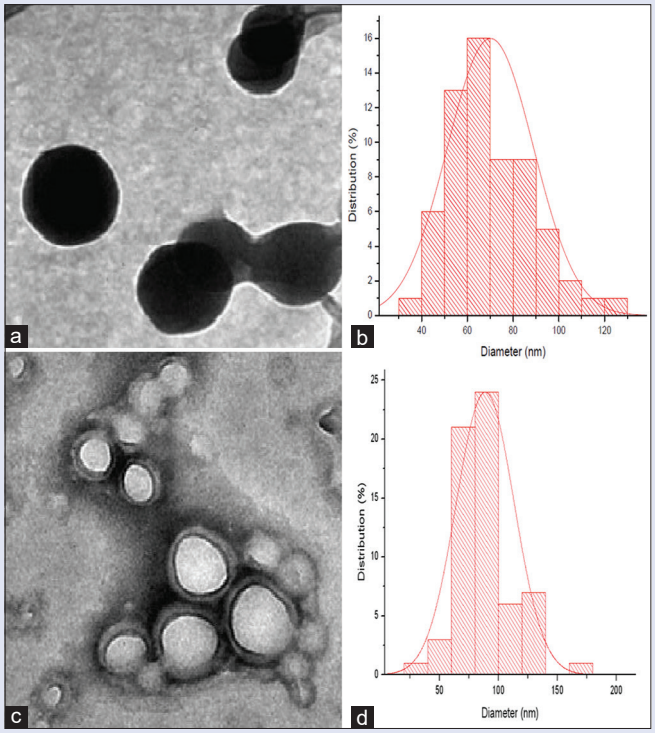

Figure 2: TEM micrograph of synthesized nanoparticles: a) morphology of PLGA-PEG *CR* F68; b) size distribution of PLGA-PEG *CR* F68 nanoparticles; c) morphology of PLGA-PEG *CR* PVAc; d) PLGA-PEG *CR* PVAc. Both nanoparticles were spherical, and the average size was higher for PLGA-PEG *CR* F68 (87.31 nm) than for PLGA-PEG *CR* PVAc (70.09 nm)

Drug release of PLGA-PEG nanoparticles synthesized with different surfactants

Comparison between both surfactants showed that the nanoparticles synthesized with PVAc achieved more than 80% drug release [Figure 4]. In contrast, nanoparticles synthesized using pluronic F68 achieved 20% drug release at this time point.

Cytotoxicity assay of PLGA-PEG *CR* nanoparticles

The IC_{50} of PLGA-PEG *CR* nanoparticles synthesized with pluronic F68 was higher in parent cells (99 µg/mL) than in tamoxifen-resistant cells (58 µg/mL). Similarly, PVAc-based nanoparticles had a higher IC_{50} value in parent cells (147 µg/mL) compared with tamoxifen-resistant cells (42 µg/mL). [Figure 5]. Both formulations exhibited cytotoxic effects particularly on resistant cells as the dose required was lower.

HER2 protein expression

Effect of *CR* PLGA-PEG F68 on HER2 protein expression was studied. Analysis indicated downregulation of protein expression in resistant cells after treatment with nanoparticles [Figure 6]. Analysis using Image Lab indicated that there was downregulation of HER2 expression by 0.6 in the resistant cells. However, the downregulation was not significant ($P = 0.19$).

Table 1: Dynamic light scattering (DLS) analysis of PLGA-PEG *CR* nanoparticles

Sample	Particle Size (nm)	PDI	Zeta Potential (mV)
PLGA-PEG *CR* F68	122.23	0.127	–2.19
PLGA-PEG *CR* PVAc	139.30	0.187	–3.44

Table 2: Percentage of EE of *CR* nanoparticles synthesized using different surfactants

Surfactant	Entrapment efficiency (%)
PVAc	60
Pluronic F68	64

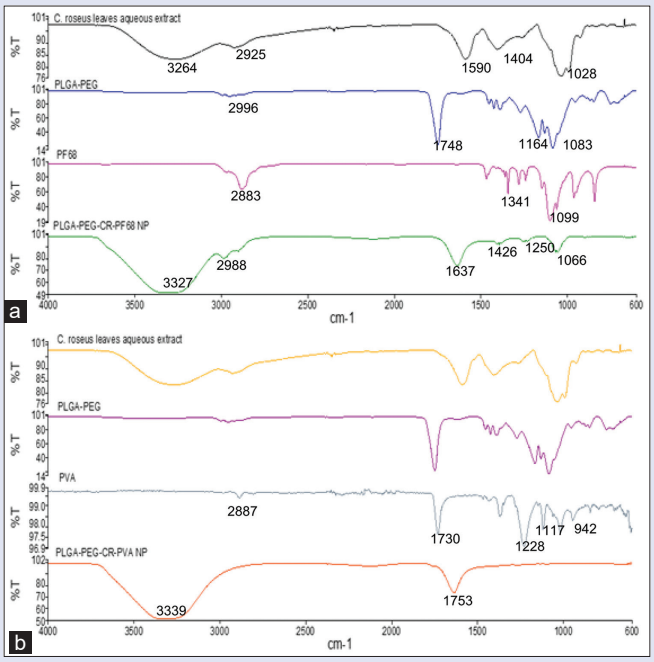

Figure 3: FTIR analysis of compositions of nanoparticles formed using PLGA-PEG to encapsulate *CR* with (a) pluronic F68 and (b) PVAc

Morphological changes before and after treatment with *CR* PLGA-PEG F68

Observation under a phase contrast microscope was done before and after treatment with nanoparticles. Findings obtained at 24 h treatment showed a reduction in the number of cells and clustering with an increase in nanoparticle concentration [Figure 7]. After 72 h of treatment, there was a prominent detachment of cells and shrinkage, which indicated apoptotic features.

DISCUSSION

CR has become an extensively studied herbal plant after the discovery of its anticancer compounds, namely, vinblastine and vincristine.[33,34] It has been studied in both animal models and cell-based models. Bioavailability of its compounds can be preserved using nanotechnology. In medicine, nanotechnology plays an important role in treatment of diseases. Nanoparticles provide a mode of transport for drug delivery.[35] Application of nanoparticles in pharmaceutical research requires modification of the surface properties to be compatible in a biological environment. Therefore, it is crucial to use biocompatible macromolecules for absorption to the surface of the nanoparticles as it is able to prevent particle aggregation under certain physico-chemical conditions.[36] Furthermore, modification of the surface with the use of non-ionic amphiphilic macromolecules (e.g., poloxamers, poloxamines, or PEG derivatives) can prevent aggregation.[37] In addition, the presence of these macromolecules can improve the drug release and also prevent partial or total denaturation. PLGA degradation is regulated by hydrolytic process, which may cause the generation of acidic oligomers and monomers that lead to an acidic microenvironment. According to a previous report, polaxamers and poloxamines are able to prevent chemical interactions between the drug and the PLGA and further neutralize the acidity generated during the course of polymer degradation.

In contrast to ongoing research about *CR* metal nanoparticles, there is limited information about the anticancer activity of *CR* extract upon encapsulation in PLGA-PEG nanoparticles. Therefore, the goal of the current study was to synthesize PLGA-based polymeric nanoparticles that contain *CR* to treat the HER2-overexpressing breast cancer cells

Ebrahim Attia *et al.* (2011)[38] previously reported that the mixed micelles synthesized using two or more than two copolymers exhibited synergistic effects for drug delivery. In another study, a TPGS-graftpoly (D, L-lactide-co-glycolide) (TPGS-g-PLGA)/Pluronic F68 mixed micelle displayed an increase in the emulsification ability, interaction of micelle-cell, and also the internalization by cells.[20] Present study used the F68 and PVAc as surfactants in the synthesis of nanoparticles and tested their effects on the characteristics of *CR* nanoparticles.

The UV-Vis spectrum indicated a maximum absorption peak at 230 nm for the positive control vinblastine, and the *CR* extract showed peaks at 235–250 nm. The maximum peak of F68 nanoparticles occurred at 230, and that of PVAc nanoparticles was detected between 200 and 245 nm. TEM analysis indicated that the nanoparticles synthesized were spherical in shape. Mean sizes of F68 and PVAc nanoparticles were 87.31 and 70.09 nm, respectively. A previous study evaluated whether melatonin could improve bioreductant capacity of silver nanoparticle synthesis using *CR* leaves.[39] Based on field emission TEM, they reported that the shape of nanoparticles to be round and size ranged from 10 to 25 nm. In another study, synthesis of *CR* leaf extract chitosan nanoparticles was done to measure the release of chloramphenicol and ketoconazole.[40] They reported that the TEM size range was between 45 and 50 nm and that the nanoparticles were polydispersed. The shape of the drug-loaded chitosan nanoparticles was hexagonal, and they had an irregular mean diameter. Furthermore, the observed insignificant increase in mean diameter was due to encapsulation and uneven drug loading on the surface of the chitosan nanoparticles. For chloramphenicol-encapsulated chitosan nanoparticles, size increased from 46 to 82 nm with 23% drug EE.

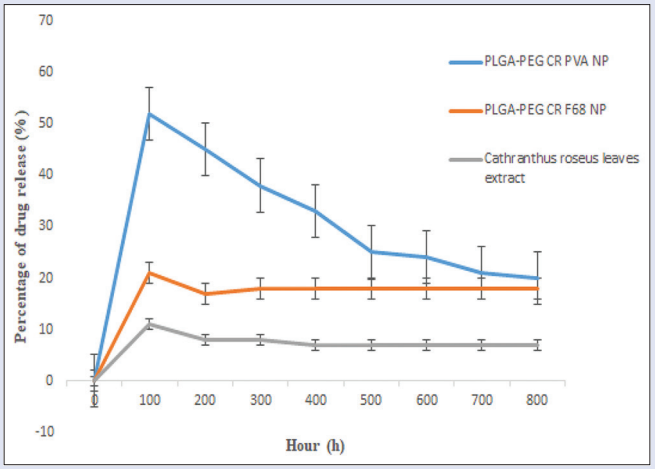

Figure 4: The release profile of nanoparticles with different surfactants

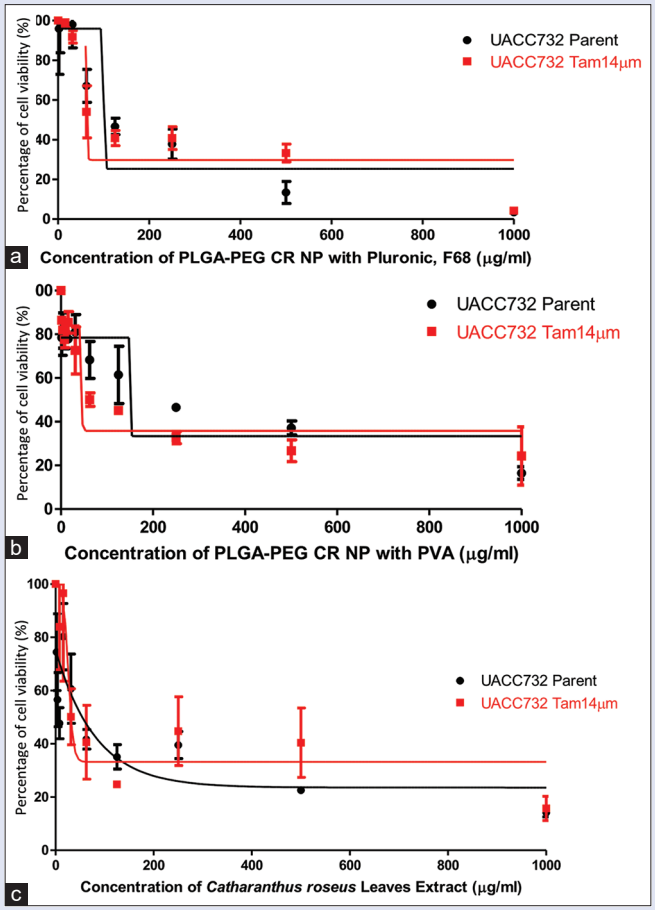

Figure 5: Cytotoxicity effects of PLGA-PEG *CR* nanoparticles synthesized with different surfactants: a) IC_{50} for the PVAc nanoparticles; b) IC_{50} for the pluronic F68 nanoparticles. Both treatments showed that tamoxifen-resistant UACC732 cell lines were more sensitive compared with the parent cell line

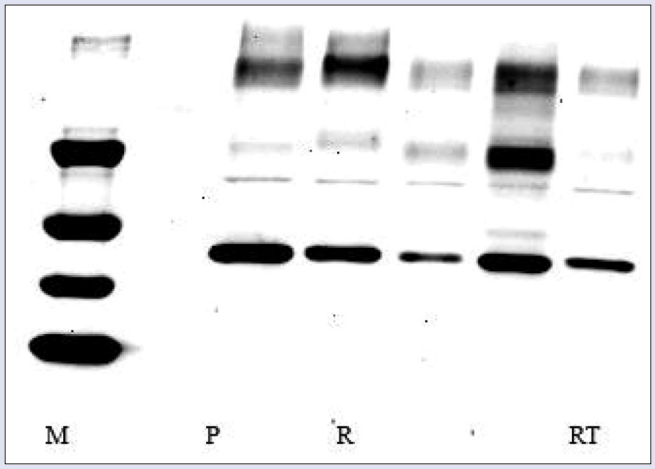

Figure 6: HER2 expression (1) Parent (2) Resistant (5) Resistant cells after treatment with CR PLGA-PEG F68 nanoparticles. Analysis was done using Western blot method using HER2 antibody. Experiments were performed in triplicates

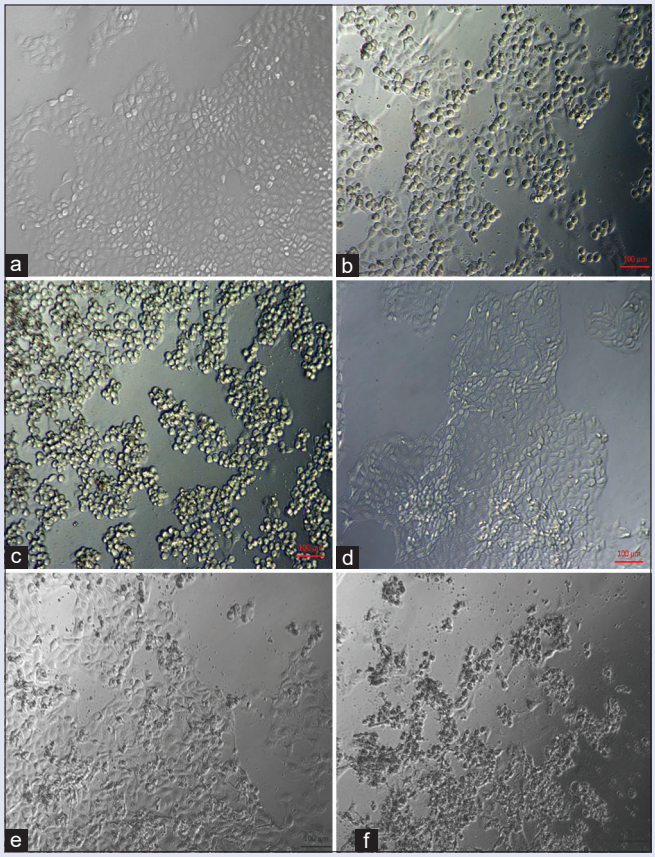

Figure 7: Morphological changes before and after treatment with PLGA-PEG *CR* nanoparticles in resistant UACC732 cells (a) untreated cells at 24 h (b) cells treated with 31 µg/mL of nanoparticles for 24 h (c) cells treated with 62/mL for 24 h (d) untreated cells at 72 h (e) cells treated with 31 µg/mL for 72 h (e) cells treated with 62 µg/mL for 72 h

Characterization of nanoparticles is an important aspect in nanotechnology development. It is focused mainly on the size of the nanoparticle and its surface charge.[35] Small nanoparticles have larger specific surfaces and may exist in aggregation or agglomeration. DLS utilizes time differences of scattered light from suspended nanoparticles under Brownian motion to determine the hydrodynamic size distribution.[35] The DLS findings showed that the nanoparticles synthesized from PVAc had a mean size of 139 nm, whereas the nanoparticles formed with F68 were smaller in mean size (122 nm). Larger sizes of CR nanoparticles were reported by Sheshadri *et al.*[39] (2015), where the average hydrodynamic diameter was 180.8 nm and PDI value of 0.438. They stated that the difference in the size of silver nanoparticles ascertained with field emission TEM and the zetasizer was consistent with previous reports.[41] In a previous study of poly-ε-caprolactone and pluronic nanoparticles, the particle size produced was 208.5 to 280.2 nm. Their PDI ranged from 0.089 to 0.169, which indicated monodispersed particles.[42] Furthermore, the size measured by the DLS method is influenced by all substances absorbed onto the particle surface, such as stabilizers, and by the thickness of the electrical double layer moving along the particle.[43] As such, the measurement provided by the DLS technique is larger than that measured by other techniques

The PVAc-based nanoparticles had a lower zeta potential value than the F68-based nanoparticles. Zeta potential is used to predict the stability of the suspension.[32] Stability of suspensions is the capacity to remain the same over a given time. It is necessary to study the physico-chemical characteristics in the optimization of new nanoparticle formulations.[44] Physical instability is contributed by the agglomeration of particles. However, this can be prevented by high surface charges or high zeta potentials. Zeta potential is determined by the nanoparticle formulation and the physicochemical properties of the nanoparticles.[45,46] Particles with high zeta potential values of either negative or positive (± 30 mV) can achieve stable suspension. This occurs through repulsion between particles that prevents their aggregation.[42] Nagaonkar *et al.* (2015)[40] reported a strong positive zeta potential when *CR* chitosan nanoparticles were used for release of chloramphenicol and ketoconazole. However, a negative value is preferred because it promotes penetration of molecules via the skin.[42]

Nanoparticle size also may vary according to the amount of the polymer in the organic phase, polarity of the solvent, and concentration of the surfactants in the aqueous phase.[42] Chawla and Amiji (2002) reported that particle size increased when pluronic F68 surfactant was removed.[47] Therefore, the presence of pluronics in the nanoparticle synthesis may act as dispersant and stabilizer.

In the current study, the chemical structures of the nanoparticles were analyzed with FTIR spectroscopy. The *CR* extract showed prominent peaks at 3264, 2995, 1590, 1404, and 1028 cm^{-1}. A previous study of silver nanoparticles generated with the water extract of *CR* leaves reported bands at 3401, 1604, 1304, and 1071 cm^{-1},[39] whereas a different study of the water extract of *CR* leaves showed major bands at 1118, 1385, and 1632 cm^{-1}.[40] For PLGA-PEG, peaks were present at 1748, 1164, and 1083 cm^{-1}. Analysis of the surfactants showed that the functional groups of F68 were at 3676, 2883, 1341, and 1099 cm^{-1}. The stretching vibration peak at 2880 is attributed to the CH_3 group.[48] PVAc alone exhibited peaks at 2887, 1730, 1228, 1117, and 942 cm^{-1}. Similar bands were previously reported for PVAc, and a band detected at 2892 cm^{-1} was attributed to CH, CH_2, and CH_3 cm^{-1} group stretching vibrations.[49] They also noted a band at 1725 cm^{-1} that was due to ester carbonyl group stretching and a band at 1218 cm^{-1} that represented the C-C(=O)-O group of PVAc. In our study, analysis of the nanoparticle formulations indicated that PLGA-PEG *CR* nanoparticles with F68 had peaks at 3327, 2988, 1637, and 1066 cm^{-1}; the peak at 3327 cm^{-1} represented the *CR* extract, and the peak at 1066 cm^{-1} represented F68. For PLGA-PEG *CR* nanoparticles with PVAc, peaks were present at 3339, 1753, and 1637 cm^{-1}; the peak at 3339 cm^{-1} represented the *CR* extract, and the

peak at 1753 cm^{-1} represented PVAc. According to previous reports, the *CR* leaf extract had infrared bands at 1118, 1354, 1500, 1524, 1543, 1548, 1632, 1793, 1736, and 1845 cm^{-1}.[40] The major band located at 1118 cm^{-1} is attributed to C-N stretching of the aliphatic amines, and the band present at 1354 cm^{-1} is due to N-O asymmetric stretching of nitro compounds. The absorption peak around 1736 cm^{-1} is attributed to C = O stretching vibrations of the carboxylic acids. The peak observed at 1632 cm^{-1} is due to the presence of N-H bending of the 1°amines.[40] These findings are supported by another report that also detected signals at 3401.2, 1604.11, 1384.59, and 1071.02 cm^{-1}, and the notable peak at 3401.2 cm^{-1} indicated stretching of the O-H band, which is found in alcohols and phenols.[39]

In the synthesis of nanoparticles surfactants are added to stabilize the nanoparticle and reduce the surface tension.[17] Coating of a polymeric surface can also help achieve stealthy properties.[50] In our study, the amount of drug released from nanoparticles was determined with UV-Vis analysis using a standard curve. The nanoparticles synthesized with PVAc showed sustained release over time compared with F68-based nanoparticles. This suggest that PVAc could be suitable to retain the activity of CR for prolonged duration. Nagaonkar *et al.* (2015)[40] reported that chloramphenicol chitosan nanoparticles exhibited initial burst of drug release during the first 5 h. Therefore, indicating that the drug absorbed onto the surface of nanoparticles had released rapidly into the medium. Subsequently, there was slow degradation of chitosan nanoparticles with the diffusion of encapsulated drug into the medium. This occurred via the pores of the nanoparticles. At 12 h, the cumulative amount of chloramphenicol released from chitosan nanoparticles was 38%. Further release of the drug was attributed to the aqueous solubility of *CR*.[40] Jawahar *et al.* (2009) reported that PLGA-pluronic F68 nanoparticles achieved almost 72% drug release.[50] They stated that smaller particles would achieve higher drug release due to their larger surface area. However, another study using PLGA-pluronic nanoparticles that were synthesized by the multiple emulsification solvent evaporation method achieved 98% release within 120 h. In our study, we tested PVAc because it is being used increasingly for anticancer applications. Recently, a PVAc-based polymeric nanoparticle was reported to inhibit the hypoxia-inducible factor-1α and reduce angiogenesis in tumor-bearing mice.[51] In another study, clofazimine-loaded PVP-b-PVAc of longer hydrophobic PVAc block length (PVP90-b-PVAc290 and PVP90-b-PVAc256) exhibit higher drug loading capacity, as well as EE, compared with shorter hydrophobic PVAc block length. The loading capacity of polymeric vesicles relies on the molecular weight of the hydrophobic block. Larger hydrophobic copolymers were reported to form thicker hydrophobic bilayer membranes and therefore they may contain more hydrophobic drug.[15]

The results also showed different responses of cells to the each of formulations of PLGA-PEG *CR* nanoparticles. Tamoxifen-resistant UACC732 cells were sensitive to PVAc nanoparticles compared with parent cells. This result could be due to prior exposure of UACC732 cells to lapatinib and trantuzumab, which may have increased their sensitivity toward the new drug. Although parent UACC 732 cells were more sensitive to pluronic F68-based PLGA-PEG CR nanoparticles. Some of the factors that may play role in the cytotoxicity effect are such as the type of surfactant coating, duration, size of nanoparticles as well the cancer cell type.[52] Further analysis on HER2 protein expression was performed with PLGA-PEG CF F68 as it exhibited prolonged sustained release. Findings obtained indicated downregulation in the expression of HER2 in resistant cells.

CONCLUSION

Finding suggest that both the formulations of PLGA-PEG *CR* nanoparticles exhibited cytotoxic effects; however, PLGA-PEG CR G68 had sustained release than PLGA-PEG CR PVAc. In addition, downregulation of HER2 expression was induced by PLGA-PEG CR F68. This warrants further investigation to confirm the targeting mechanism of the nanoparticles in HER2-overexpressed breast cancer cells.

Acknowledgments

Ministry of Education, Malaysia.

Financial support and sponsorship

This work was supported by the Fundamental Research Grant Scheme from the Ministry of Education, Malaysia with project code FRGS/1/2016/SKK13/USM/02/1.

Conflicts of interest

There are no conflicts of interest.

REFERENCES

1. Slamon D, Clark G, Wong S, Levin W, Ullrich A, McGuire W. Human breast cancer: Correlation of relapse and survival with amplification of the HER-2/neu oncogene. Science 1987;235:177-82.
2. Pondé N, Brandão M, El-Hachem G, Werbrouck E, Piccart M. Treatment of advanced HER2-positive breast cancer: 2018 and beyond. Cancer Treat Rev 2018;67:10-20.
3. Kumar B, Jalodia K, Kumar P, Gautam HK. Recent advances in nanoparticle-mediated drug delivery. J Drug Deliv Sci Tech 2017;41:260-8.
4. Hepokur C, Kariper İA, Mısır S, Ay E, Tunoğlu S, Ersez MS, *et al.* Silver nanoparticle/capecitabine for breast cancer cell treatment. Toxicol *In Vitro* 2019;61:104600.
5. Nascimento TG, Da Silva PF, Azevedo LF, Da Rocha LG, de Moraes Porto ICC, e Moura TFAL, *et al.* Polymeric Nanoparticles of Brazilian red propolis extract: Preparation, characterization, antioxidant and leishmanicidal activity. Nanoscale Res Lett 2016;11:301.
6. Hadinoto K, Sundaresan A, Cheow WS. Lipid–polymer hybrid nanoparticles as a new generation therapeutic delivery platform: A review. Eur J Pharm Biopharm 2013;85:427-43.
7. Yang X, Zhang X, Ma Y, Huang Y, Wang Y, Chen Y. Superparamagnetic graphene oxide–Fe 3 O 4 nanoparticles hybrid for controlled targeted drug carriers. J Mater Chem 2009;19:2710-4.
8. Keck CM, Müller RH. Nanotoxicological classification system (NCS)–A guide for the risk-benefit assessment of nanoparticulate drug delivery systems. Eur J Pharm Biopharm 2013;84:445-8.
9. Chowdhury SM, Lalwani G, Zhang K, Yang JY, Neville K, Sitharaman B. Cell specific cytotoxicity and uptake of graphene nanoribbons. Biomaterials 2013;34:283-93.
10. Anderson JM, Shive MS. Biodegradation and biocompatibility of PLA and PLGA microspheres. Adv Drug Deliv Rev 1997;28:5-24.
11. Gentile P, Chiono V, Carmagnola I, Hatton PV. An overview of poly(lactic-co-glycolic) acid (PLGA)-based biomaterials for bone tissue engineering. Int J Mol Sci 2014;15:3640-59.
12. Astete CE, Sabliov CM. Synthesis and characterization of PLGA nanoparticles. J Biomater Sci Polym Edition 2006;17:247-89.
13. Tyrrell ZL, Shen Y, Radosz M. Fabrication of micellar nanoparticles for drug delivery through the self-assembly of block copolymers. Prog Polym Sci 2010;35:1128-43.
14. Maeda H, Wu J, Sawa T, Matsumura Y, Hori K. Tumor vascular permeability and the EPR effect in macromolecular therapeutics: A review. J Controlled Release 2000;65:271-84.
15. Bailly N, Thomas M, Klumperman B. Poly(N-vinylpyrrolidone)-block-poly (vinyl acetate) as a drug delivery vehicle for hydrophobic drugs. Biomacromolecules 2012;13:4109-17.
16. Patra A, Satpathy S, Shenoy AK, Bush JA, Kazi M, Hussain MD. Formulation and evaluation of mixed polymeric micelles of quercetin for treatment of breast, ovarian, and multidrug resistant cancers. Int J Nanomedicine 2018;13:2869-81.
17. Menon JU, Kona S, Wadajkar AS, Desai P, Vadla A, Nguyen KT. Effects of surfactants on the properties of PLGA nanoparticles. J Biomed Mater Res A 2012;100:1998-2005.
18. Batrakova EV, Kabanov AV. Pluronic block copolymers: Evolution of drug delivery concept from inert nanocarriers to biological response modifiers. J Controlled Release 2008;130:98-106.

19. Oh KT, Bronich TK, Kabanov AV. Micellar formulations for drug delivery based on mixtures of hydrophobic and hydrophilic Pluronic® block copolymers. J Controlled Release 2004;94:411-22.
20. Kerleta V, Andrlik I, Schneider M, Franke T, Wirth M, Gabor F. Pluronic® F-68 Enhances the Nanoparticle-Cell Interaction. Sci Pharm 2009;77:179.
21. Jannesari M, Varshosaz J, Morshed M, Zamani M. Composite poly (vinyl alcohol)/poly (vinyl acetate) electrospun nanofibrous mats as a novel wound dressing matrix for controlled release of drugs. Int J Nanomedicine 2011;6:993.
22. Park KR, Nho YC. Preparation and characterization by radiation of hydrogels of PVA and PVP containing Aloe vera. J Appl Polym Sci 2004;91:1612-8.
23. Sadato A, Taki W, Ikada Y, Nakahara I, Yamashita K, Matsumoto K, *et al.* Experimental study and clinical use of poly (vinyl acetate) emulsion as iquid embolisation material. Neuroradiology 1994;36:634-41.
24. Malarvizhi GL, Retnakumari AP, Nair S, Koyakutty M. Transferrin targeted core-shell nanomedicine for combinatorial delivery of doxorubicin and sorafenib against hepatocellular carcinoma. Nanomedicine 2014;10:1649-59.
25. Pernas S, Tolaney SM. HER2-positive breast cancer: New therapeutic frontiers and overcoming resistance. Ther Adv Med Oncol 2019;11:1758835919833519.
26. Ghozali SZ, Ismail MN, Ahmad NHJM JoM and sciences H. Characterisation of silver nanoparticles using a standardised catharanthus roseus aqueous extract. Malaysian J Med Health Sci 2018;14:120-5.
27. Vega E, Egea MA, Valls O, Espina M, García ML. Flurbiprofen loaded biodegradable nanoparticles for ophtalmic administration. J Pharm Sci 2006;95:2393-405.
28. Desai R, Mankad V, Gupta SK, Jha PK. Size distribution of silver nanoparticles: UV-visible spectroscopic assessment. Nanosc Nanotechnol Lett 2012;4:30-4.
29. Tang J, Zhang R, Guo M, Shao L, Liu Y, Zhao Y, *et al.* Nucleosome-inspired nanocarrier obtains encapsulation efficiency enhancement and side effects reduction in chemotherapy by using fullerenol assembled with doxorubicin. Biomaterials 2018;167:205-15.
30. Siti Z, Seoparjoo A, Shahrul H. Lipoproteins modulate growth and P-glycoprotein expression in drug-resistant HER2-overexpressed breast cancer cells. Heliyon 2019;5:e01573.
31. Ramos AP. 4-Dynamic light scattering applied to nanoparticle characterization. In: Da Róz AL, Ferreira M, de Lima Leite F, Oliveira ON, editors. Nanocharacterization Techniques. William Andrew Publishing; 2017. p. 99-110.
32. Retamal Marín RR, Babick F, Hillemann L. Zeta potential measurements for non-spherical colloidal particles – Practical issues of characterisation of interfacial properties of nanoparticles. Colloids Surf A: Physicochem Eng Aspects 2017;532:516-21.
33. Zhang X-N, Liu J, Liu Y, Wang Y, Abozeid A, Yu Z-G, *et al.* Metabolomics analysis reveals that ethylene and methyl jasmonate regulate different branch pathways to promote the accumulation of terpenoid indole alkaloids in *Catharanthus roseus*. J Nat Prod 2018;81:335-42.
34. Kulkarni R, Baskaran K, Jhang T. Breeding medicinal plant, periwinkle [*Catharanthus roseus* (L) G. Don]: A review. Plant Genet Resour 2016;14:283-302.
35. Xu R. Progress in nanoparticles characterization: Sizing and zeta potential measurement. Particuology 2008;6:112-5.
36. Santander-Ortega MJ, Jódar-Reyes AB, Csaba N, Bastos-González D, Ortega-Vinuesa JL. Colloidal stability of Pluronic F68-coated PLGA nanoparticles: A variety of stabilisation mechanisms. Colloid Interface Sci 2006;302:522-9.
37. Moghimi SM, Hunter AC. Poloxamers and poloxamines in nanoparticle engineering and experimental medicine. Trends Biotechnol 2000;18:412-20.
38. Ebrahim Attia AB, Ong ZY, Hedrick JL, Lee PP, Ee PLR, Hammond PT, *et al.* Mixed micelles self-assembled from block copolymers for drug delivery. Curr Opin Colloid Interface Sci 2011;16:182-94.
39. Sheshadri S, Sriram S, Balamurugan P, Anupriya R, Princy SA, Brindha P, *et al.* Melatonin improves bioreductant capacity and silver nanoparticles synthesis using *Catharanthus roseus* leaves. RSC Adv 2015;5:47548-54.
40. Nagaonkar D, Gaikwad S, Rai M. *Catharanthus roseus leaf* extract-synthesized chitosan nanoparticles for controlled *in vitro* release of chloramphenicol and ketoconazole. Colloid Polym Sci 2015;293:1465-73.
41. Singh R, Shedbalkar UU, Wadhwani SA, Chopade BA. Bacteriagenic silver nanoparticles: Synthesis, mechanism, and applications. App Microbiol Biotechnol 2015;99:4579-93.
42. Do Nascimento TG, Da Silva PF, Azevedo LF, Da Rocha LG, de Moraes Porto ICC, e Moura TFAL, *et al.* Polymeric Nanoparticles of Brazilian red propolis extract: Preparation, characterization, antioxidant and leishmanicidal activity. Nanoscale Res Lett 2016;11:301.
43. Tomaszewska E, Soliwoda K, Kadziola K, Tkacz-Szczesna B, Celichowski G, Cichomski M, *et al.* Detection limits of DLS and UV-Vis spectroscopy in characterization of polydisperse nanoparticles colloids. J Nanomater 2013;2013:60.
44. Ohshima H. Electrical Phenomena at Interfaces and Biointerfaces: Fundamentals and Applications in Nano-, Bio-, and Environmental Sciences. John Wiley & Sons; 2012.
45. Delgado AV, González-Caballero F, Hunter RJ, Koopal LK, Lyklema J. Measurement and interpretation of electrokinetic phenomena. J Colloid Interface Sci 2007;309:194-224.
46. Zembala M. Electrokinetics of heterogeneous interfaces. Adv Colloid Interface Sci 2004;112:59-92.
47. Chawla JS, Amiji MM. Biodegradable poly (ε-caprolactone) nanoparticles for tumor-targeted delivery of tamoxifen. Int J Pharm 2002;249:127-38.
48. Cai Y, Sun Z, Fang X, Fang X, Xiao F, Wang Y, *et al.* Synthesis, characterization and anti-cancer activity of Pluronic F68–curcumin conjugate micelles. Drug Deliv 2016;23:2587-95.
49. Pal MK, Gautam J. Effects of inorganic nanofillers on the thermal degradation and UV-absorbance properties of polyvinyl acetate. J Therm Anal Calorim 2013;111:689-701.
50. Jawahar N, Venkatesh DN, Sureshkumar R, Senthil V, Ganesh GNK, Vinoth P, *et al.* Development and characterization of PLGA-nanoparticles containing carvedilol. J Pharm Sci Res 2009;1:123-8.
51. Wang T, Meng J, Wang C, Jia M, Ge Y, Xie L, *et al.* Inhibition of murine breast cancer metastases by hydrophilic As4S4 nanoparticles is associated with decreased ROS and HIF-1α downregulation. Front Oncol 2019;9:333.
52. Aliakbari M, Mohammadian E, Esmaeili A, Pahlevanneshan Z. Differential effect of polyvinylpyrrolidone-coated superparamagnetic iron oxide nanoparticles on BT-474 human breast cancer cell viability. Toxicol *In Vitro* 2019;54:114-22.